

A NEW INTERPOLATED MODEL FOR PREFORM COMPACTION IN THE VACUUM ASSISTED RESIN TRANSFER MOLDING PROCESS

John M. Bayldon^{1,3} and Isaac M. Daniel²

¹ *Department of Civil and Environmental Engineering, Northwestern University,
2145 Tech Drive, #CAT330 Evanston, IL 60201, USA*

² *Walter P. Murphy Professor of Civil and Environmental and Mechanical Engineering,
Northwestern University 2145 Tech Drive, #CAT326 Evanston, IL 60201, USA*

Email: imdaniel@northwestern.edu

³ *Corresponding author's Email: j-bayldon@northwestern.edu*

SUMMARY: In Vacuum Assisted Resin Transfer Molding (VARTM) the resin flow rate is significantly affected by the preform thickness, this affects both the infusion and compaction phases of the process, and it is therefore essential to properly model the preform deformation through the entire process cycle. A typical process cycle for VARTM involves applying vacuum to compact the preform, and infusion, during which the preform becomes saturated with resin and then partly relaxes, and a final compaction after the inlet is sealed and the resin pressure reduces one more to the final vacuum level. Current available models include the non-linear compaction behavior, and the time dependant creep and relaxation behaviors of the preform, however these models do not typically account for the preform behavior when the compaction pressure is partially reduced, and then reapplied. In this paper, the preform compaction process is studied for two materials over the range of compaction cycles present in typical VARTM processes. Their behaviors are compared to existing compaction models, and a modification of the existing models is proposed to account for both partial unloading and reloading. This gives a good prediction for the more complex preform compaction cycles found in the VARTM process.

KEYWORDS: Vacuum Assisted Resin Transfer Molding (VARTM), preform compaction, process modeling

INTRODUCTION

In liquid composite molding the resin flow is affected by the pressure gradients and the preform permeability. In RTM the preform thickness is controlled by the tool cavity, however in VARTM the thickness is controlled by the fluid pressure and the preform compaction behavior. Because the permeability is governed by the preform compaction, the relationship between pressure, saturation and preform compaction is an essential part of modeling the VARTM process. The

fiber compaction process is complex, and has been studied for a considerable time in the textile industry. It is almost immediately apparent that the compaction process is non-linear, since an uncompacted textile will offer almost no resistance to compaction, whereas at the limit of compaction we can expect the stiffness to be close to the stiffness of a solid mass of the material making up the fiber.

Existing models for the compaction of the preform in composite processing have typically concentrated on the initial fabric compaction, although the effect of repeated compactions and the hysteresis observed between the loading and unloading behavior have been noted [1]. One reason for this is that in the traditional composite manufacturing methods, the fiber stack is compacted monotonically from its initial state to the final consolidated thickness, and hence the main interest has been in the first load application. In textile processing, the effect of multiple compactions has been studied in more detail, though typically the models developed have been for randomly oriented fibers (typical in processing of wool). The earliest physical model [2] was developed over 50 years ago by Van Wyk, who was studying the compaction of wool and calculated the stiffness by assuming that the deformation was solely the result of fibers bending between contact points. Making additional assumptions about the distance between contact points and orientation of the fibers allowed the following expression to be derived:

$$p = KEV_f^3(V^3 - V_0^3) \quad (1)$$

where p is the applied pressure, E the elastic modulus of the fibers, V_f the volume of material in the system (the fiber mass divided by the fiber density), V the current volume, and V_0 the volume at zero pressure. K is an empirical constant required due to the simplifying assumptions used in deriving the model. Although this model could be used to fit the loading part of the compaction curve for wools, it has several significant weaknesses, including its inability to account for the different behavior on unloading, and its inability to account for the observed permanent deformation of the fiber stack. For composites it has a further disadvantage in that it does not deal with aligned fibers. Gutowski et al. [3, 4] incorporated some of the same ideas for their model of the transverse compression of aligned fiber bundles. This model was developed for the compaction of pre-preg and hence considered a lubricated fiber bundle (neglecting any losses associated with fiber slippage):

$$p = \frac{3\pi E}{\beta^4} \frac{\sqrt{\frac{V_f}{V_0}} - 1}{\left(\sqrt{\frac{V_a}{V_f}} - 1\right)^4} \quad (2)$$

This simple model can capture the behavior of even complex preforms adequately, despite being designed solely for aligned fiber arrays. Unlike the simpler empirical power law proposed by Robitaille [1, 5] it has the advantage of having no singularities over the range of use ($V_0 < V_f < V_a$). Robitaille models the compaction as

$$p = aV_f^b \quad (3)$$

where a and b are empirical constants. The singularity occurs in the preform thickness which is inversely proportional to the volume fraction. Since $p=0$ implies $V_f=0$, this gives an infinite thickness, which is problematic for any VARTM model. All these models consider deformation only at the fiber level, and assume either random fibers or aligned fibers. If we wish to consider

woven fabrics, a considerably more complex physical model is required. Chen and Chou [6] created a comprehensive finite element model for plain weave fabrics, however this type of modeling requires significant effort and the results are typically not applicable to variations in the fabric type. In their model they develop a unit cell for the fabric and use experimentally determined pressure profiles at the contact points between fabric layers and assumed pressure profiles at the contact points between tows within each layer. These models do not show significantly better performance than the simpler models of Gutowski [3] and Robitaille [1, 5, 7], though they have the advantage of being calculated from geometrical measurements of the fabric's architecture. In addition none of the models discussed so far can account for the hysteresis behavior of fabrics, the permanent deformation, or the effects of cyclic loading.

In the textile industry literature, it has been noted that there are two types of loss mechanism present in the compaction of random assemblies of fiber. Both time dependent (viscous type) and time independent (frictional type) loss mechanisms are seen. In liquid composite molding, Bickerton [8-13] has studied the time dependent effects of preform loading. Bickerton observed both a loading rate effect and a relaxation after the end of loading. From this he proposed a viscoelastic model, which works acceptably for monotonic compaction as found in RTM and compression RTM, however it does not work well for the slow cyclic compaction observed in VARTM, largely because the dissipative viscous part of the behavior is not sufficiently recoverable on unloading.

The Compaction Process in VARTM

In the VARTM process the compaction pressure on the preform is usually assumed to be a pressure loading from the balance between the fluid inside the vacuum bag and the atmospheric pressure outside the bag. The local gradients in thickness are considered small enough to assume

$$P_c = P_{atm} - P_{fluid} = -\sigma_{zz} \tag{4}$$

where p_c is the compressive pressure on the preform, p_{atm} the atmospheric pressure (~101Kpa) and p_{fluid} the pressure of the resin or air inside the bag, $-\sigma_{zz}$ is the compressive stress on the bag surface.

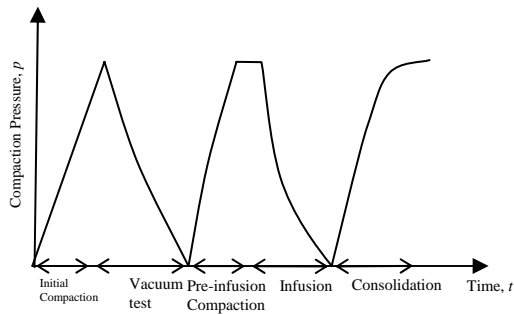


Fig. 1 Schematic of preform compaction stages.

Table 1 Preform compaction stages

1.	preform consolidation under vacuum
2.	preform compaction released as part of vacuum integrity testing
3.	preform reconsolidation prior to infusion
4.	infusion starts, as flow front passes point on interest, the consolidation pressure slowly decreases
5.	end of infusion, inlet closed, fluid pressure slowly decreases, resulting in an increase in compaction pressure

During a typical process cycle the vacuum bag will be evacuated, thereby compressing the preform. One or more vacuum leak tests will be carried out, each of which will involve a partial or full decompaction of the preform. Before infusion, the bag is evacuated again and the resin

flow is allowed to start. The pressure drop in the dry part of the preform is very small compared to the pressure drop in the resin saturated part, so at any point the preform remains compressed at 1 atmosphere until the resin passes, after which the fluid pressure rises gradually, thus reducing the preform compaction. At the end of infusion (when the resin has reached the outlet) the inlet is closed and the fluid pressure through most of the system gradually decreases. Fig. 1 and Table 1 show a typical preform compaction pressure cycle. To properly model VARTM, we therefore need a model to describe the behavior of the preform after the first initial compaction cycle, including a description of the behavior after partial unloading and reloading to full compaction.

Proposed Model

Various models have been proposed for the non-linear elastic behavior observed. To simplify model development further we assume that the viscoelastic behavior is small and normalize the model using the maximum pressure p_{atm} (101 kPa) and the volume fraction at the maximum pressure V_f^* defining the following normalized parameters for pressure and volume fraction respectively:

$$\beta = \frac{P_c}{P_{atm}}, \quad \alpha = \frac{V_f}{V_f^*} \quad (5)$$

For the loading model described here we use a modified form of Gutowski's model Eqn. (2) normalized using the maximum compaction pressure applied $p_{max} = p_{atm}$

$$\beta_l = \frac{(\sqrt{\alpha_a} - 1)^4 \left(1 - \sqrt{\frac{\alpha}{\alpha_0}}\right)}{\left(1 - \sqrt{\frac{1}{\alpha_0}}\right) \left(\sqrt{\frac{\alpha_a}{\alpha}} - 1\right)^4} \quad (6)$$

For the unloading behavior a simple empirical relationship is used to fit the curve:

$$\beta_u = \frac{(\alpha_a - \alpha)^n - (\alpha_a - \alpha_0)^n}{(\alpha_a - 1)^n - (\alpha_a - \alpha_0)^n} \quad (7)$$

The constant terms in these equations are set to ensure that $\beta(\alpha = \alpha_0) = 0$ and $\beta(\alpha = 1) = 1$. We note from experimental observation that, as long as the load is restricted to the load limit of the first cycle, any subsequent load history will be bounded by these two envelope curves, and the subscripts l , u refer to the loading and unloading behavior for the second and subsequent full loading cycles. The lack of a unique value of α for any value of β (and vice versa) is a problem for modeling. However, if we assume (as appears to be true from experimental observations) that the curves for loading from intermediate value form a non intersecting family of curves, we can at least develop a model for the incremental unloading and loading behavior from any point as long as we know both α and β .

Reloading from Partial Unloading

A simple interpolation model for the reloading from partial unloading would take the form:

$$\begin{aligned}
\beta^*(\alpha, \alpha^*) &= \beta_l(\alpha) - f(\alpha, \alpha^*)(\beta_l(\alpha) - \beta_u(\alpha)) \\
f(\alpha = \alpha^*, \alpha^*) &= 1 \\
f(\alpha = 1, \alpha^*) &= 0
\end{aligned} \tag{8}$$

where $\beta_l^*(\alpha, \alpha^*)$ is the normalized pressure for loading from α^* , having unloaded from $\alpha=1$ to α^* , f is an interpolation function. The interpolation scheme used here is based on a linear reduction in the difference between β and β_l during reloading.

$$\begin{aligned}
\beta^{**}(\alpha, \alpha^*) &= \beta_l(\alpha) - f(\alpha, \alpha^*)(\beta_l(\alpha^*) - \beta_u(\alpha^*)) \\
f(\alpha = \alpha^*, \alpha^*) &= 1, f(\alpha = 1, \alpha^*) = 0
\end{aligned} \tag{9}$$

A schematic of this is shown in

Fig. 2. Converting the final form (13) to a more useable one, we have

$$p = p_{\max} \left(\beta_l(\alpha) - \left(\frac{1-\alpha}{1-\alpha^*} \right) (\beta_l(\alpha^*) - \beta_u(\alpha^*)) \right) \tag{10}$$

Differentiating this gives

$$\frac{\partial p}{\partial \alpha} = p_{\max} \left(\frac{\partial \beta_l}{\partial \alpha} + \frac{\beta_l}{1-\alpha} \right) + \frac{p}{1-\alpha} \tag{11}$$

Unloading from Partial Loading

For the unloading from partial loading we use a similar interpolation method, but this time based on a linear reduction in the difference between the current volume fraction and the expected volume fraction during unloading from full compaction.

$$\alpha = \frac{\alpha_u + k\alpha_0}{(1+k)}, \quad k = \frac{\alpha_u - \alpha_0}{\alpha^* - \alpha_0} \tag{12}$$

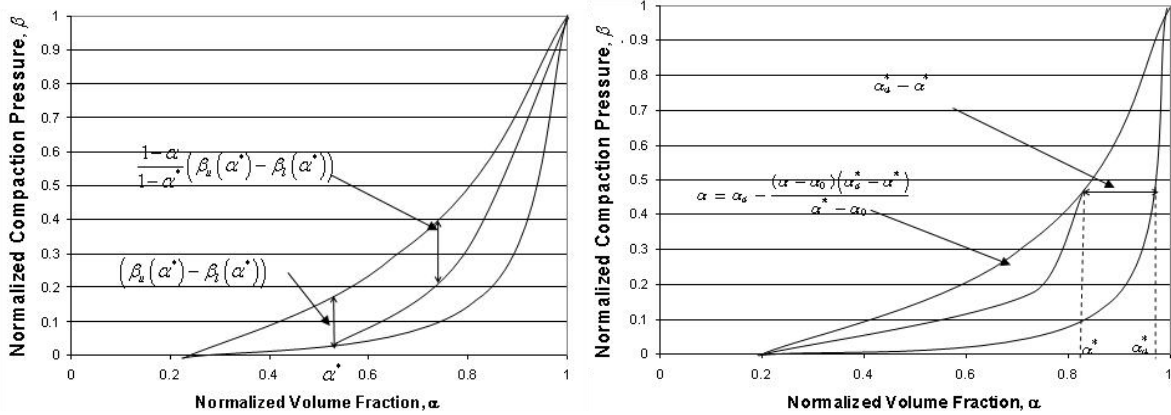


Fig. 2 Schematics of the models.

where:

$$\alpha_u = \alpha_a - [\beta_u ((\alpha_a - 1)^n - (\alpha_a - \alpha_0)^n) + (\alpha_a - \alpha_0)^n]^{1/n} \quad (13)$$

EXPERIMENTAL EVALUATION OF PROPOSED COMPACTION MODEL

Two glass fiber reinforcement fabrics were used in these evaluation trials, Hexcel 7500 style plain weave glass and OCF8610 Continuous Filament (Random) Mat. The ECG fibers used in both fabrics are e-glass with a diameter of between 8.9 μm and 10.1 μm . The experimental program involved compressing stacks of preforms in a hydraulic testing machine. The experimental set up is shown in Fig. 3. The preforms were compressed between a 2.5cm thick, 25cm diameter aluminum disk and a support plate. The compaction forces were recorded using the machine load cell or a smaller independently recorded load cell (0-8.9KN) mounted between the cross head and the test plate.

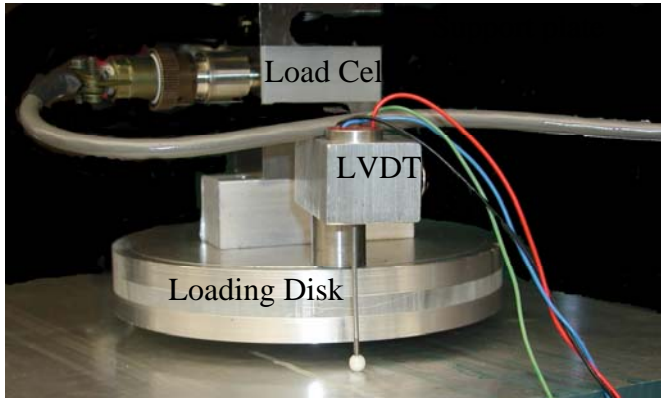


Fig. 3 Test Jig.

The preform thickness was recorded using a linear voltage displacement transducer (LVDT) recording the separation between the loading disk and the flat support plate. Using the machine cross-head displacement distorts the results significantly due to the small thickness of the specimens. The loading rate was chosen to be slow enough to minimize the time dependent effects observed. Two different materials were studied, a plain weave (PW) E-glass (7500 style) and a glass continuous filament mat (CFM, OCF8610).

Two types of experiment were carried out, partial loading and partial unloading experiments. In both types, an initial loading cycle was used in which the fabric was loaded to 101KPa, immediately unloaded to the original thickness, and then reloaded to 101KPa. For the partial loading experiments the preform was fully unloaded, and subsequently a series of partial reloading cycles were carried out. For the partial unloading experiments the preform was unloaded to various intermediate states before reloading to full compaction.

The plain weave was reloaded to the same thickness at each maximum load point, the CFM however, showed noticeable deformation at each cycle and was therefore loaded to a slightly increased thickness. To limit systematic errors in the measurements, the intermediate unloading points were not sequential.

Lubricated preforms were saturated with water. Preliminary experiments indicated no difference in the results between water and viscous oil (silicone oil 0.2Pas) when the tests with oil were conducted sufficiently slowly. The benefit of using water is that the viscosity is sufficiently low that no significant fluid pressure is developed in the water during testing. This removes the need to correct for the fluid pressure developed as required when a higher viscosity fluid is used [14].

COMPARISON WITH EXPERIMENTAL RESULTS

The experimental testing was carried out using a 16 ply preform of the plain weave fabric and a 4 ply preform of the CFM. The preforms were loaded in a hydraulic testing machine, to an applied pressure of 1atm. The preform was then unloaded completely, reloaded to 1 atm, and then subsequently unloaded to several intermediate pressures, on each unloading it was reloaded to 1 atm. The envelope curves were fitted to several models and the most suitable models were selected. The fitting constants used are shown in Table 2.

Table 2 Parameters used for envelope curves

	Plain Weave				CFM			
	Loading		Unloading		Loading		Unloading	
	Wet	Dry	Wet	Dry	Wet	Dry	Wet	Dry
m	4	4	-1.7	10	4	4	-2.0	-2.0
α_0	0.776	0.811	0.776	0.811	0.224	0.224	0.14	0.224
α_a	1.28	1.25	1.02	1.25	1.49	2.04	1.05	1.05

The envelope curves indicated that the Gutowski and Robitaille models both fit the loading curves for the plain weave fabric fairly well; however neither can be made to fit the unloading behavior well without substantial modification. The main difficulty being the initial slope at the start of unloading, this is considerably steeper than either model. This is not surprising since both models were developed to model the loading behavior only. For the unloading behavior the best fit was obtained using the empirical power law from Eqn. 7. We do note however that while the α_0 values for the Gutowski model are physically realistic for this fabric, the equivalent values used in the Empirical Power law model have no physical meaning, and must be separately fitted.

The same comparisons also hold for the CFM material, though the viscoelastic behavior, which is ignored in this analysis, does distort the results. Having established the unloading and loading envelope behaviors we can now investigate the effectiveness of the proposed interpolation model for intermediate loading conditions. Fig. 4 and 5 show the partial reloading behavior for the two fabrics in the two conditions along with the modeled envelope curves and the interpolated model.

CONCLUSIONS

The results shown here for reloading after partial unloading are in good agreements with the interpolated model for both CFM and plain weave fabrics. The results for unloading after partial loading (Fig. 5) do not give such good agreements, although the interpolation gives much better results than relying on the unloading or loading models alone.

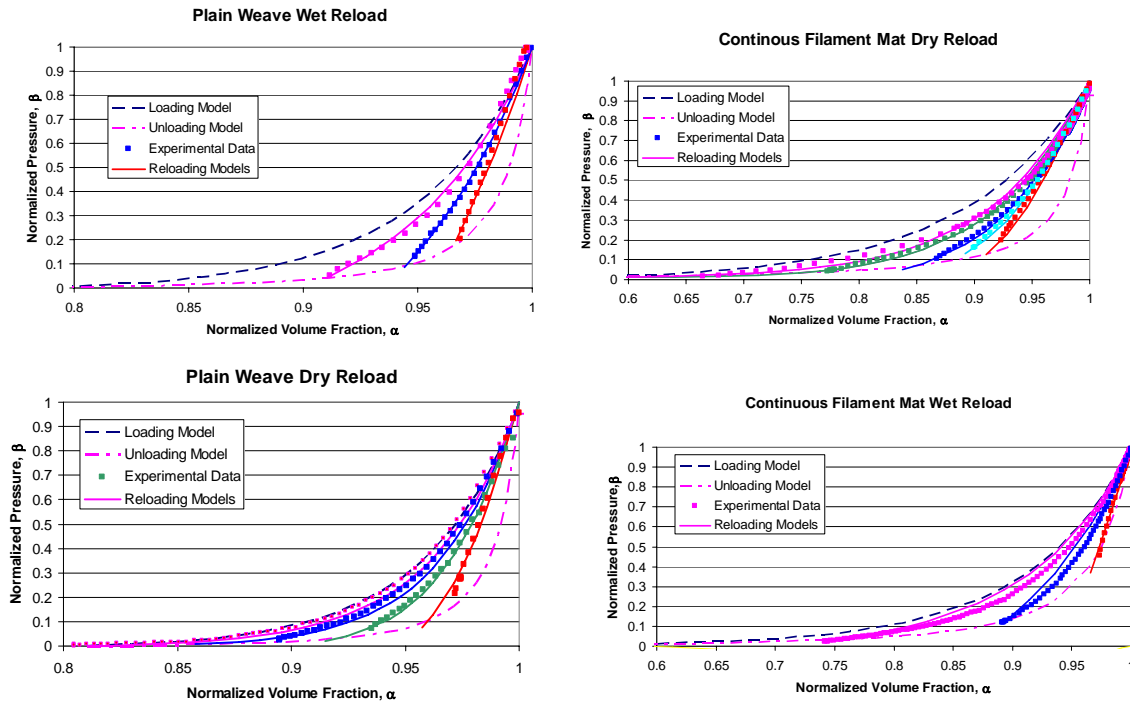


Fig. 4 Behavior on reloading after partial unloading.

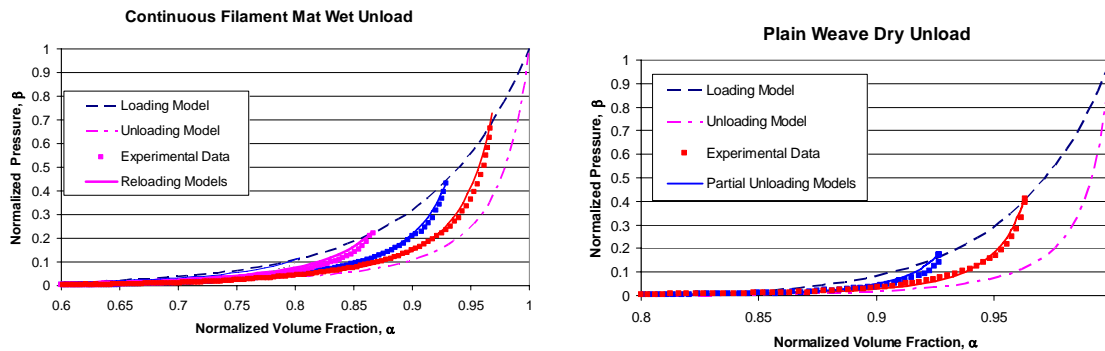


Fig. 5 Behavior of preforms on unloading after partial loading.

The compaction models developed here provides an acceptable fit for the data measured on the hydraulic testing machine (Instron), and provide a significantly better model for the compaction behavior than the models typically described in the literature. Most VARTM flow models described in the literature, if they specify the compaction model at all, simply refer to the unloading behavior of the wet preform. If the incorrect unloading model is used the thickness data will be very poorly reproduced, since an unloading curve taken from a higher initial loading pressure will fall entirely outside the envelope curve for a lower initial pressure.

ACKNOWLEDGMENTS

The work described here was funded by the Office of Naval Research through Dr Ignacio Perez.

REFERENCES

1. Robitaille, F. and R. Gauvin, "Compaction of Textile Reinforcements for Composites Manufacturing. I: Review of Experimental Results", *Polymer Composites*, 1998. 19(2): p. 198-216.
2. Van Wyk, C., "Note on the Compressibility of Wool", *Journal of the Textile Institute*, 1946. 37: p. T285-T292.
3. Gutowski, T.G., T. Morigaki, and Z. Cai, "The Consolidation of Laminate Composites", *Journal of Composite Materials*, 1987. 21(2): p. 172-188.
4. Gutowski, T.G., "Advanced Composites Manufacturing", 1997, New York: John Wiley and Sons.
5. Robitaille, F. and R. Gauvin, "Compaction of Textile Reinforcements for Composites Manufacturing. II: Compaction and Relaxation of Dry and H₂O-Saturated Woven Reinforcements", *Polymer Composites*, 1998. 19(5): p. 543-557.
6. Chen, B.X. and T.W. Chou, "Compaction of Woven-Fabric Preforms in Liquid Composite Molding Processes: Single-Layer Deformation", *Composites Science and Technology*, 1999. 59(10): p. 1519-1526.
7. Robitaille, F. and R. Gauvin, "Compaction of Textile Reinforcements for Composites Manufacturing. III: Reorganization of the Fiber Network", *Polymer Composites*, 1999. 20(1): p. 48-61.
8. Bickerton, S. and M.Z. Abdullah, "Modeling and Evaluation of the Filling Stage of Injection/Compression Moulding", *Composites Science and Technology*, 2003. 63(10): p. 1359-1375.
9. Bickerton, S. and S.G. Advani, "Experimental Investigation and Flow Visualization of the Resin-Transfer Mold-Filling Process in a Non-Planar Geometry", *Composites Science and Technology*, 1997. 57(1): p. 23-33.
10. Bickerton, S. and S.G. Advani, "Characterization and Modeling of Race-Tracking in Liquid Composite Molding Processes", *Composites Science and Technology*, 1999. 59(15): p. 2215-2229.
11. Bickerton, S., et al., "Experimental Analysis and Numerical Modeling of Flow Channel Effects in Resin Transfer Molding", *Polymer Composites*, 2000. 21(1): p. 134-153.
12. Bickerton, S., M.J. Buntain, and A.A. Somashekar, "The Viscoelastic Compression Behavior of Liquid Composite Molding Preforms", *Composites Part a-Applied Science and Manufacturing*, 2003. 34(5): p. 431-444.
13. Bickerton, S., et al., "Investigation of Draping and its Effects on the Mold Filling Process during Manufacturing of a Compound Curved Composite Part", *Composites Part a-Applied Science and Manufacturing*, 1997. 28(9-10): p. 801-816.
14. Kelly, P.A., R. Umer, and S. Bickerton, "Viscoelastic Response of Dry and Wet Fibrous Materials during Infusion Processes", *Composites Part a-Applied Science and Manufacturing*, 2006. 37(6): p. 868-873.